Publishing House
AKAPIT

COMPUTER METHODS IN MATERIALS SCIENCE

Informatyka w Technologii Materiałów

Vol. 8, 2008, No. 3

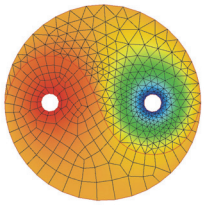

A FINITE ELEMENT ANALYSIS OF THE SUPERPLASTIC BLOW-FORMING IN AN AWL-SHAPED DIE WITH TITANIUM ALLOY

DYI-CHENG CHEN, HSIN-NENG WANG

Department of Industrial Education and Technology,
National Changhua University of Education, Changhua 500, Taiwan, R.O.C.
Corresponding Author: dyi3510@ms46.hinet.net (D.-C. Chen)

Abstract

This study employs commercial DEFORM^{TM} 3D finite element analysis software to simulate the superplastic blow-forming of Ti-6Al-4V titanium alloy sheet into triangular, square and conical awl-shaped dies. In performing the simulations, the die model is constructed using 3D solid elements and the titanium sheet is assumed to be a rigid-plastic material with homogeneous and isotropic properties. The simulations focus specifically on the respective effects of the shear friction, the sheet thickness, and the damage value criterion on the distributions of the effective stress, effective strain, damage, and deformation velocity within the blow-formed products. Overall, the simulation results confirm the suitability of DEFORM^{TM} 3D software for modeling the superplastic blow-forming of titanium alloy sheets into awl-shaped dies with various geometries.

Key words: superplastic blow-forming, awl-shaped dies, damage, titanium alloy

1. INTRODUCTION

The term 'superplasticity' describes the capability of certain polycrystalline materials such as 8090 Al-Li alloy, Ti-6Al-4V alloy and so forth, to undergo extensive tensile plastic deformation prior to failure under specific temperature and strain-rate conditions. The characteristics of superplasticity, namely a low flow stress and a high elongation, have led to the development of a variety of 'superplastic forming' (SPF) processes such as forging, extrusion, blow-forming, and so on (Miller and White, 1988; Al-Naib and Duncan, 1970). Senthil Kumar et al. (2006) investigated the superplastic deformation behavior of AA7475 aluminum alloy during its blow-forming into a hemispherical die and compared the results obtained using a simple theoretical model with those generated by ABAQUS FE code. Yarlagadda et al. (2002) performed FE simulations of the superplastic forming of Al-Ti alloys and used the results obtained for the deformed shape, the stress-strain distribution and the thickness evolution across the facets of the fully-formed surface to optimize the processing conditions and to predict the forming time. Hambli et al. (2001) presented 2D and 3D finite element models for predicting the optimum pressure cycle law, the deformed shape, the strain rate distribution and the thickness evolution during superplastic forming processes. The validity of the pressure prediction algorithm used in the numerical solution procedure was confirmed by comparing the numerical results with the experimental observations. Hwang et al. (2002, 2003) utilized commercial DEFORM^{TM} FE software to investigate the pressurization profile and sheet thickness distribution of 8090 Al-Li sheets blow-formed into closed ellipcylindrical and rectangular dies, respectively. Lee and Huh (1999) applied FE code to analyze the su-

 ISSN 1641-8581

perplastic-forming / diffusion-bonding (SPF/DB) of four-sheet sandwich components. Wang et al. (2008) investigated the superplastic deformation of Ti-6Al-2Zr-1Mo-1V titanium alloy, and found that MaxmSPD (maximum m superplasticity deformation) processing yielded a significant improvement in the superplasticity of the titanium alloy compared to that achieved using a conventional SPD process with a cyclically changing strain rate.

In a previous study, the current group utilized the Taguchi design method to identify the processing parameters which optimized the thickness distribution of Ti-6Al-4V titanium alloy blow-formed into an ellip-cylindrical die (Chen et al., 2007). In the current study, commercial DEFORM^{TM} 3D FE software is used to investigate the plastic deformation behavior of Ti-6Al-4V alloy sheet blow-formed into awl-shaped dies with three different geometric configurations, namely triangular, square and conical. The simulations assume the Ti-6Al-4V alloy to be a rigid-plastic material with homogeneous and isotropic properties, and construct the various die models using 3D solid elements. For each awl-shaped die, the simulations are designed to clarify the effects of the shear friction, sheet thickness and damage value criterion on the effective stress, effective strain, critical damage and deformation velocity within the blow-formed product.

2. FINITE-ELEMENT FORMULATION AND MATERIAL CONSTITUTIVE EQUATION

According to Kim and Yang (1985), the FE formulation for the rigid-plastic deformation of an engineering material subject to work hardening has the form

$$\int_{V^w}(\bar{\sigma}+\alpha\Delta t\dot{\bar{\varepsilon}}H')\delta\dot{\bar{\varepsilon}}dV+K\int_{V^w}\dot{\varepsilon}_v\delta\dot{\varepsilon}_v dV-\int_{S_f^w}(f_i+\alpha\Delta f_i)\delta v_i dS=0, \quad (1)$$

where $\bar{\sigma}=\sqrt{(3/2)\sigma_{ij}^{'}\sigma_{ij}^{'}}$, $\dot{\bar{\varepsilon}}=\sqrt{(2/3)\dot{\varepsilon}_{ij}\dot{\varepsilon}_{ij}}$ and $\dot{\varepsilon}_v=\dot{\varepsilon}_{ii}$. Additionally, K, $\sigma_{ij}^{'}$, H' and α are the penalty constant, the deviatoric stress, the strain-hardening rate and the work-hardening constant ($0\le\alpha\le1$), respectively, while V^w and S_f^w are the volume and tractional boundary surface of the workpiece, respectively.

The DEFORM^{TM} 3D FE simulations performed in this study are based on a flow formulation approach using an updated Lagrangian procedure. The nonlinear equations in the FE software are solved using a combined direct iteration method / Newton-Raphson scheme. In the solution procedure, the direct iteration method is used to generate a suitable initial estimate, and the Newton-Raphson method is then applied to obtain a rapid convergence to the final solution. The iterative solution procedure continues until the following termination criteria are achieved: a velocity error norm of $\|\Delta\mathbf{v}\|/\|\mathbf{v}\|\le0.005$ and a force error norm of $\|\Delta F\|/\|F\|\le0.05$, where $\|\mathbf{v}\|$ is $(\mathbf{v}^T\mathbf{v})^{1/2}$.

The deformation behavior of a superplastic alloy such as that considered in the present study is governed by the relationship between the von Mises equivalent (effective) stress and the equivalent (effective) strain rate, and is generally expressed as follows:

$$\bar{\sigma}=K\dot{\bar{\varepsilon}}^m\varepsilon^n. \quad (2)$$

For simplicity, the equivalent flow stress is assumed to vary as the following function of the strain rate:

$$\bar{\sigma}=K\dot{\bar{\varepsilon}}^m, \quad (3)$$

where K is the material coefficient, and includes the combined effect of both the equivalent strain and the grain size; and m is the strain-rate sensitivity.

Various formulations have been proposed for modeling the damage induced in engineering materials during their ductile deformation (Klocke et al., 2002). The simulations performed in this study consider six different damage criteria, namely:

1. Normalized Cockcroft & Latham (C&L):

$$\int_0^{\bar{\varepsilon}_f}\frac{\sigma_{\max}}{\bar{\sigma}}d\bar{\varepsilon}=C; \quad (4)$$

2. Cockcroft & Latham:

$$\int_0^{\bar{\varepsilon}_f}\sigma_{\max}d\bar{\varepsilon}=C; \quad (5)$$

3. McClintock:

$$\int_0^{\bar{\varepsilon}_f}\left[\frac{\sqrt{3}}{2(1-n)}\sinh\left\{\frac{\sqrt{3}}{2}(1-n)\frac{\sigma_1+\sigma_2}{\bar{\sigma}}\right\}+\frac{3}{4}\frac{\sigma_1-\sigma_2}{\bar{\sigma}}\right]d\bar{\varepsilon}=C; \quad (6)$$

4. Freudenthal:

$$\int F(deformation)d\bar{\varepsilon}=C; \quad (7)$$

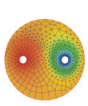

5. Ayada:

$$\int_0^{\bar{\varepsilon}_f} \frac{\sigma_m}{\bar{\sigma}} d\bar{\varepsilon} = C; \tag{8}$$

6. Brozzo:

$$\int_0^{\bar{\varepsilon}_f} \frac{2\sigma_{\max}}{3(\sigma_{\max} - \sigma_m)} d\bar{\varepsilon} = C; \tag{9}$$

where $\sigma_{\max}$ is the maximum ductile stress, σ_1 and σ_2 are the principal stresses, $\bar{\sigma}$ is the effective stress, $\bar{\varepsilon}$ is the effective strain, σ_m is the hydraulic compressive stress (mean stress), n is the strain-hardening exponent, $\bar{\varepsilon}_f$ is the effective fracture strain, F is a material deformation function, and C is the damage value of the material.

3. RESULTS AND DISCUSSION

In simulating the superplastic blow-forming of the Ti-6Al-4V alloy sheet into the three awl-shaped dies, the following assumptions are made: (1) the die is a rigid body; (2) the alloy sheet is a rigid-plastic material with homogeneous and isotropic properties; and (3) the friction factor between the titanium sheet and the die remains constant throughout the duration of the blow-forming process.

As shown in table 1, the simulation parameters are specified as follows: an initial sheet thickness (t) of 1.0 mm or 1.5 mm; a shear friction factor (m) of 0.2, 0.3 or 0.4; a die entry radius (R) of 3 mm; a die height of 50 mm; a die dimension (L) of 100 mm; a processing temperature (T) of 800°C; a strain rate of 0.1 s^{-1}; and an arc radius (Rc) of 2 mm. The major dimensions of the triangular, square and conical awl dies are depicted schematically in Figs. 1(a)~1(d).

The geometry and processing parameters considered in each of the current simulation runs are summarized in table 2. Note that for each simulation, the initial pressure and pressure increase applied after 10 steps are both assigned values of 0.5 MPa. The two right-most columns of the table indicate the damage value criterion applied in each simulation run and the corresponding maximum damage value, respectively. Overall, the results reveal that for given values of the geometry and processing parameters, the square awl-shaped die yields the minimum damage within the blow-formed product, while the triangular awl-shaped die yields the greatest damage. In other words, the square die suppresses the formation of stress fractures during the blow-forming of the Ti-6Al-4V alloy sheet. In addition, observing the results presented for simulation runs #12 and #19~23, respectively, it can be seen that for a blow-forming process conducted using a conical die with constant geometry and processing conditions, the Freudenthal criterion predicts the greatest damage within the deformed product, whilst the Ayada criterion predicts the minimum damage.

(a) Illustrates of dimension (b) Triangular awl-shaped

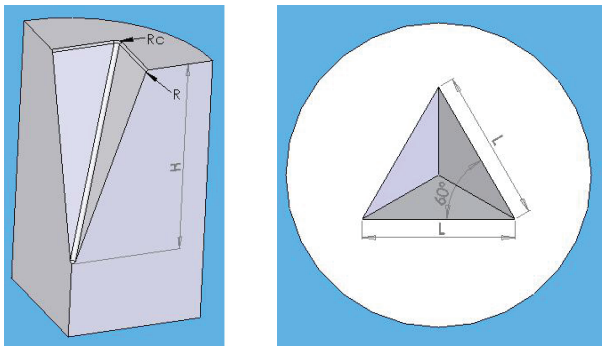

(c) Square awl-shaped (d) Cone shape

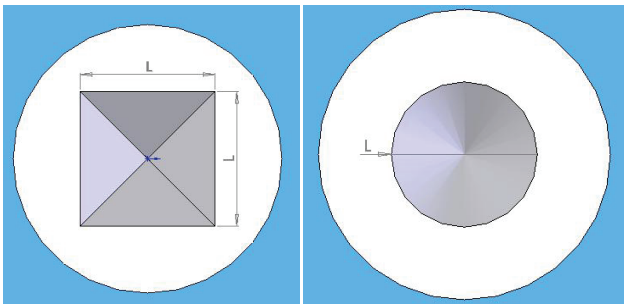

Fig. 1. *Illustration of major dimensions of each awl-shaped die.*

Table 1. *Constant parameters used in superplastic blow-forming simulations for all awl-shaped dies.*

Materials	Initial sheet thickness (t)	Shear friction factor (m)	Die entry radius (R)	Die height (H)	Die dimension (L)	Temperature (T)	Stain rate	Arc radius (Rc)
Titanium (Ti-6Al-4V)	1 mm, 1.5 mm	0.2, 0.3, 0.4	3 mm	50 mm	100 mm	800℃	0.1 (1/s)	2 mm

Table 2. *Summary of geometry parameters, processing conditions, damage value criteria and maximum damage values for each simulation run.*

Factors / No.	Awl-shaped die	Thickness of sheet (mm)	Shear friction factor (m)	Initial press(MPa)	Increasing pressure after 10 steps (MPa)	Judgment of fracture	Maximum damage value
1	triangular awl-shaped	1	0.2	0.5	0.5	Normalized C& L criterion	3.13
2	square awl-shaped	1	0.2	0.5	0.5	Normalized C& L criterion	0.78
3	cone shaped	1	0.2	0.5	0.5	Normalized C& L criterion	1.85
4	triangular awl-shaped	1	0.3	0.5	0.5	Normalized C& L criterion	3.55
5	square awl-shaped	1	0.3	0.5	0.5	Normalized C& L criterion	0.901
6	cone shaped	1	0.3	0.5	0.5	Normalized C& L criterion	1.17
7	triangular awl-shaped	1	0.4	0.5	0.5	Normalized C& L criterion	3.44
8	square awl-shaped	1	0.4	0.5	0.5	Normalized C& L criterion	0.998
9	cone shaped	1	0.4	0.5	0.5	Normalized C& L criterion	1.13
10	triangular awl-shaped	1.5	0.2	0.5	0.5	Normalized C& L criterion	5.22
11	square awl-shaped	1.5	0.2	0.5	0.5	Normalized C& L criterion	1.48
12	cone shaped	1.5	0.2	0.5	0.5	Normalized C& L criterion	2.36
13	triangular awl-shaped	1.5	0.3	0.5	0.5	Normalized C& L criterion	3.67
14	square awl-shaped	1.5	0.3	0.5	0.5	Normalized C& L criterion	1.48
15	cone shaped	1.5	0.3	0.5	0.5	Normalized C& L criterion	2.93
16	triangular awl-shaped	1.5	0.4	0.5	0.5	Normalized C& L criterion	4.11
17	square awl-shaped	1.5	0.4	0.5	0.5	Normalized C& L criterion	1.43
18	cone shaped	1.5	0.4	0.5	0.5	Normalized C& L criterion	1.51
19	cone shaped	1.5	0.2	0.5	0.5	Ayada	1.11
20	cone shaped	1.5	0.2	0.5	0.5	Brozzo	3.05
21	cone shaped	1.5	0.2	0.5	0.5	Cockcroft & Latham	440
22	cone shaped	1.5	0.2	0.5	0.5	Freudenthal	747
23	cone shaped	1.5	0.2	0.5	0.5	McClintock	8.56

t=1 mm, R=3 mm, H=50 mm, L=100 mm, T=800°C, Rc=2 mm, m=0.2

(a) before forming

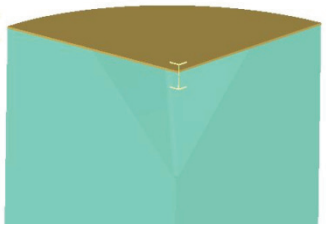

(b) during forming

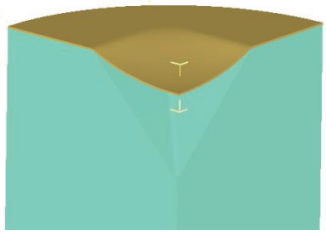

(c) after forming

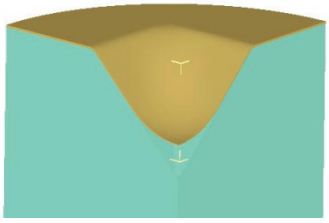

Fig. 2. *Snapshots of simulated blow forming of Ti-6Al-4V sheet into square die under simulation conditions #2.*

Figures 2(a)~2(c) present snapshots of the simulated blow-forming of the Ti-6Al-4V alloy sheet into the square awl-shaped die. Note that due to the symmetry of the die, only one-quarter of the sheet / die model is presented. As shown, the simulation was performed using the following parameters and conditions: t (sheet thickness) = 1 mm, R (die entry radius) = 3 mm, H (die height) = 50 mm, L (die dimension) = 100 mm, m (shear friction factor) = 0.2, T (processing temperature) = 800°C, Rc (arc radius) = 2 mm, and strain rate = $0.1s^{-1}$. In addition, an assumption was made that the titanium sheet was firmly attached to the perimeter of the die such that no metal flowed from the periphery regions of the sheet into the die cavity during the forming process. Figures 3(a)~3(c) illustrate the appearance of the blow-formed products produced using the triangular, square and conical dies, respectively. Note that in every case, the simulations were performed using the following geometry parameters and processing conditions: t = 1.5 mm, R = 3 mm, H = 50 mm, L = 100 mm, m = 0.2, T = 800°C, Rc = 2 mm, and strain rate = 0.1 s^{-1}. As expected from the damage values presented in table 2, the products produced using the square and conical awl-shaped dies have a smooth, flawless appearance, whereas that produced using the triangular die shows signs of fracture cracking in the tip region.

t=1.5 mm, R=3 mm, H=50 mm, L=100 mm, T=800°C, Rc=2 mm, m=0.2

(a)Simulated No. 10 (triangular awl-shaped)

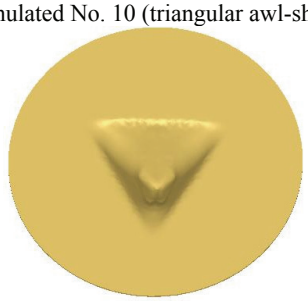

(b) Simulated No.11 (square awl-shaped)

(c) Simulated No.12 (cone shaped)

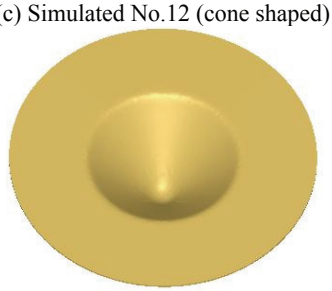

Fig. 3. *Appearance of blow-formed Ti-6Al-4V products produced using three different awl-shaped dies.*

Figures 4(a)~4(c) present the damage distributions in the blow-formed Ti-6Al-4V products produced in the triangular, square and conical dies, respectively, using the same geometry and processing conditions as those considered in figure 3. Observing the three figures, it is seen that in every case, the maximum damage is induced in the tip region of the blow-formed product. Moreover, comparing the three figures, it is evident that the minimum damage is induced in the product produced using the square die, while the maximum damage is induced in the product produced using the triangular die.

t=1.5 mm, R=3 mm, H=50 mm, L=100 mm, T=800°C, Rc=2 mm, m=0.2

(a) Simulated No. 10 (triangular awl-shaped)

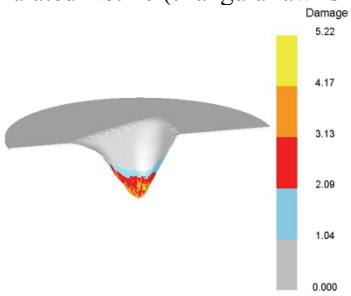

(b) Simulated No. 11 (square awl-shaped)

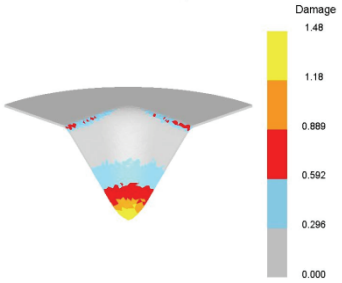

(c) Simulated No. 12 (cone shaped)

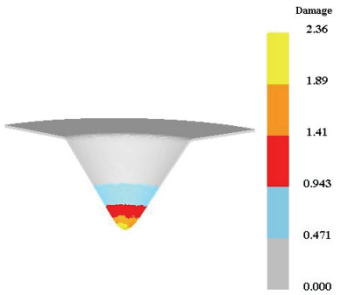

Fig. 4. *Distribution of damage in blow-formed Ti-6Al-4V products produced using three different awl-shaped dies.*

t=1.5 mm, R=3 mm, H=50 mm, L=100 mm, T=800°C, Rc=2 mm, m=0.2

(a) Simulated No. 10 (triangular awl-shaped)

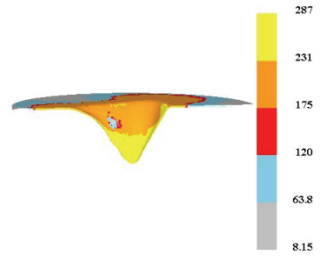

(b) Simulated No. 11 (square awl-shaped)

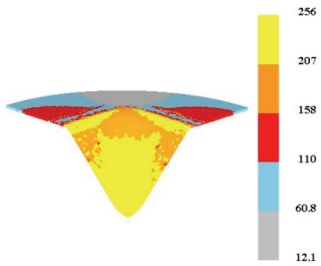

(c) Simulated No. 12 (cone shaped)

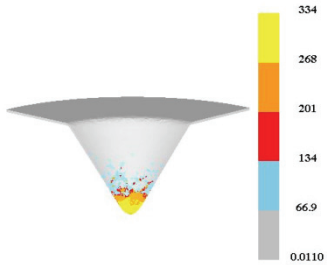

Fig. 5. *Distribution of effective stress in blow-formed Ti-6Al-4V products produced using three different awl-shaped dies (unit: MPa).*

t=1.5 mm, R=3 mm, H=50 mm, L=100 mm, T=800°C, Rc=2 mm, m=0.2

(a) Simulated No. 10 (triangular awl-shaped)

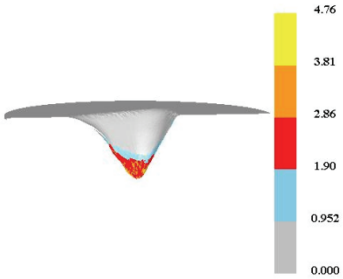

(b) Simulated No. 11 (square awl-shaped)

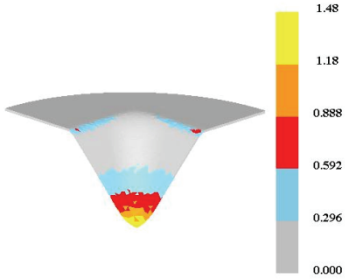

(c) Simulated No. 12 (cone shaped)

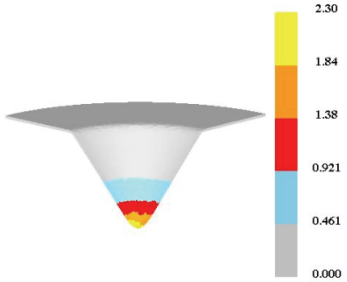

Fig. 6. *Distribution of effective strain in blow-formed Ti-6Al-4V products produced using three different awl-shaped dies.*

Figures 5(a)~5(c) show the distribution of the effective stress in each of the blow-formed products produced using the geometry parameters and processing conditions considered in figure 3. As expected, the square die induces the minimum effective stress within the blow-formed product, while the triangular induces the greatest effective stress.

Figures 6(a)~6(c) illustrate the distribution of the effective strain in the three blow-formed Ti-6Al-4V products produced using the geometry parameters and processing conditions considered in figure 3. Comparing the three figures, it is evident that the minimum and maximum effective strains are produced in the products formed using the square die and the triangular die, respectively.

Finally, figures 7(a)~7(b) show the distribution of the deformation velocity in the Ti-6Al-4V products blow-formed in the triangular and square awl-shaped dies using the same parameters and conditions as those considered in figure 3. From inspection, the results show that the maximum velocity in the triangular die (0.107 mm/sec) is significantly higher than that in the square die (0.00343 mm/sec) and therefore accounts for the greater effective stress, effective strain and damage values observed in the triangular blow-formed products.

t=1.5 mm, R=3 mm, H=50 mm, L=100 mm, T=800°C,
Rc=2 mm, m=0.2

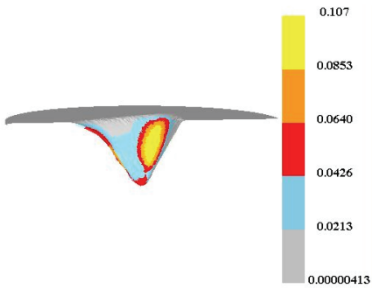

(a) Simulated No. 10 (triangular awl-shaped)

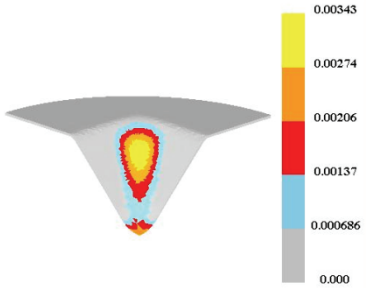

(b) Simulated No. 11 (square awl-shaped)

Fig. 7. *Distribution of deformation velocity in blow-formed Ti-6Al-4V products produced using two different awl-shaped dies (units: mm/sec).*

4. CONCLUSIONS

This study has utilized commercial DEFORM™ 3D FE software to analyze the plastic deformation behavior of Ti-6Al-4V titanium alloy during its superplastic blow-forming into triangular, square and conical awl-shaped dies. The simulation results support the following major conclusions: (1) the greatest values of the effective stress and effective strain are induced in the triangular die, while the minimum values of the effective stress and effective strain are induced in the square die; (2) the square die induces the minimum amount of damage to the blow-formed Ti-6Al-4AV alloy sheet, while the triangular die induces the maximum damage; and (3) the products blow-formed using the square and conical dies have a smooth, flawless appearance, while those produced in the triangular die have fracture cracks in the tip region.

REFERENCES

1. Al-Naib, T.Y.M., Duncan, J.L., 1970, Superplastic Metal Forming, Int. J. Mech. Sci. 12, 463-477.
2. Chen, D.C., Lin, J.Y., Jheng, M.W., Chen, J.M., 2007, Design of Titanium Alloy Superplastic Blow-forming in Ellip-cylindrical Die Using Taguchi Method, Proceedings of the 35th International MATADOR Conference, 105-109, Taipei, July 18-20.
3. Hambli, R., Potiron, A., Guerin, F., Dumon, B., 2001, Numerical Pressure Prediction Algorithm of Superplastic Forming Processes Using 2D and 3D Models, Journal of Materials Processing Technology, 112, 83-90.
4. Hwang, Y.M., Lay, H.S. Huang, J.C., 2002, Study on Superplastic Blow-forming of 8090 Al-Li Sheets in an Ellip-cylindrical Closed-die, International Journal of Machine Tools & Manufacture, 42, 1363-1372.
5. Hwang, Y.M., Lay, H.S., 2003, Study on Superplastic Blow-forming in a Rectangular Closed-die, Journal of Materials Processing Technology, 140, 426-431.
6. Kim, Y.J., Yang, D.Y., 1985, A Formulation for Rigid-plastic Finite Element Method Considering Work-hardening Effect, International Journal of Mechanical Sciences, 27, 487.
7. Klocke, F., Breuer, D., Raedt, H., 2002, Proceeding of the 7th ICTP, Advanced Technology of Plasticity, 1, 721-728, Yokohama.
8. Lee, K.S., Huh, H., 1999, Simulation of Superplastic Forming/diffusion Bonding with Finite-element Analysis Using the Convective Coordinate System, Journal of Materials Processing Technology, 89-90, 92-98.
9. Miller, Q.S., White, J., in Superplasticity in Aerospace, Heikkenen, H.C., McNelley (Eds.), T.R., AIME, Warrendate, PA, 1988, 211-217.
10. Senthil Kumar, V.S., Viswanathan, D., Natarajan, S., 2006, Theoretical Prediction and FEM Analysis of Superplastic Forming of AA7475 Aluminum Alloy in a Hemispherical Die, Journal of Materials Processing Technology, 173, 247-251.

11. Yarlagadda, P.K.D.V., Gudimetla, P., Adam, C., 2002, Finite Element Analysis of High Strain Rate Superplastic Forming (SPF) of Al-Ti alloys, Journal of Materials Processing Technology, 130-131, 469-476.
12. Wang, G.C., Fu, M.W., Cao, C.X., Dong, H.B., Geng, Q.D., 2008, Research on Superplasticity Deformation of Ti-alloy Ti-6Al-2Zr-1Mo-1V, Proceedings of the 8th Asia Pacific Conference on Materials Processing, 951-957, Guilin-Guangzhou, June 15-20.

KSZTAŁTOWANIE METODĄ DMUCHU STOPU TYTANU W MATRYCACH O KSZTAŁCIE OSTROSŁUPA METODĄ ELEMENTÓW SKOŃCZONYCH

Streszczenie

W niniejszej pracy wykorzystano komercyjną wersję programu metody elementów skończonych DEFORM™ 3D do symulacji kształtowania blach ze stopu tytanu Ti-6Al-4V metodą dmuchu w matrycy stożkowej o podstawie trójkąta, kwadratu i okręgu. W pracy wykorzystano pełne trójwymiarowe elementy dyskretyzujące rozpatrywany materiał. Ponadto założono sztywno plastyczny model materiału z jednorodnymi oraz izotropowymi własnościami. Symulacja dostarczyła informacji na temat zależności pomiędzy tarciem, grubością próbki i wartościami kryterium pękania a uzyskanymi wartościami intensywności naprężeń, odkształceń, uszkodzeń i prędkością odkształcenia. Uzyskane wyniki symulacji potwierdziły przydatność programu DEFORM™ 3D do modelowania kształtowania metodą dmuchu blach ze stopu tytanu w matrycach o kształcie ostrosłupa.

Submitted: September 9, 2008
Submitted in a revised form: December 5, 2008
Accepted: December 12, 2008